*microorganisms*

MDPI

*Article*

# Spent Mushroom Substrate Improves the Performance of *Trichoderma harzianum* for the Biocontrol of Rice Blast

**Ning Liu †, Xiaocan Chen †, Haohai Zhang, Ming Ying * and Meitong Li ***

Tianjin Key Laboratory of Organic Solar Cells and Photochemical Conversion, College of Chemistry and Chemical Engineering, Tianjin University of Technology, Tianjin 300384, China; liuning@stud.tjut.edu.cn (N.L.); chencan61@stud.tjut.edu.cn (X.C.); haohai24@stud.tjut.edu.cn (H.Z.)

* Correspondence: ym@tjut.edu.cn (M.Y.); tjutlmt@email.tjut.edu.cn (M.L.)

† These authors contributed equally to this work.

## Abstract

*Trichoderma harzianum*, a beneficial rhizosphere ascomycete, is widely used for the control of a variety of plant diseases. However, powdered *T. harzianum* inoculant (PTH) suffers from poor root-colonization capacity and variable biocontrol efficacy, which limits its field application. In this study, an antagonistic *T. harzianum* strain TH10 was isolated from marine algal sediments. Using spent mushroom substrate (SMS) as the carrier for TH10, we developed an SMS-based *T. harzianum* inoculant (STH) for rice blast control. Scanning electron microscopy (SEM) revealed dense fungal mycelial networks on root surfaces of STH-treated rice, and these hyphae were presumed to be *T. harzianum*. At the three-leaf, tillering, and jointing stages, shoot height and root length of *Pyricularia oryzae*-infected rice treated with STH increased by 0.56–26.48% and 25.02–29.51% relative to those treated with PTH, respectively. Furthermore, STH increased the 1000-grain weight by 23.70% relative to the untreated control and by 12.99% relative to PTH, and improved grain number per panicle and panicle weight. STH exhibited a biocontrol efficacy of 51.34 ± 6.39% under greenhouse conditions, and reduced panicle-blast severity to 14.60 ± 2.68%. Transcriptomic data suggest that SMS may promote cuticular lipid biosynthesis in root tissues, and these lipids might in turn serve as carbon sources for *T. harzianum*. Most defense-related pathways, including phenylpropanoid biosynthesis, effector-triggered immunity (ETI), and MAPK cascades, were significantly upregulated in rice blast-infected shoots. These pathways may be associated with the accumulation of the immune-signaling molecules abscisic acid (ABA) and salicylic acid (SA), a response accompanying enhanced disease resistance in rice.

**Keywords:** *Trichoderma harzianum*; spent mushroom substrate; biological control; *Pyricularia oryzae*

Check for updates

Academic Editor: Gustavo Santoyo

Received: 29 August 2026
Revised: 15 October 2026
Accepted: 16 October 2026
Published: 22 October 2026

**Copyright:** © 2026 by the authors. Licensee MDPI, Basel, Switzerland. This article is an open access article distributed under the terms and conditions of the Creative Commons Attribution (CC BY) license.

## 1. Introduction

Rice (*Oryza sativa*), one of the most important cereal crops, serves as the staple food for more than half of the global population, with Asia dominating both its total output and consumption [1]. However, rice cultivation is constantly challenged by diverse pathogens, among which *Pyricularia oryzae* poses one of the most destructive threats [2]. Rice blast varies in severity among rice-producing countries, and moderate-to-severe epidemics are frequent in China's rice-growing regions in most years [3]. It is estimated that rice blast causes annual yield losses of 10–30%, and the lost grain can meet the annual food

requirements of around 60 million people. When environmental conditions favor pathogen outbreaks, rice blast may cause 70–80% grain loss and even complete yield failure [4]. Beyond yield reduction, rice blast severely degrades grain quality, posing a serious threat to global food security and sustainable rice production [5].

*Pyricularia oryzae*, a hemibiotrophic fungus belonging to the phylum Ascomycota, mainly exists in its anamorphic state in nature [6–8]. Its lightweight, wind-dispersed conidia can infect rice leaves, stems and panicles. They adhere to leaf cuticles, germinate, and form melanized appressoria that generate high intracellular turgor pressure to penetrate host epidermal cells. Subsequently, necrotic lesions develop on host tissues, and the pathogen produces new asexual conidia. These spores spread to neighboring rice plants, completing the infection cycle and causing substantial yield losses [9]. Although chemical control can achieve satisfactory efficacy, it often causes environmental pollution and accelerates the emergence of fungicide resistance [10,11]. Therefore, biological control has attracted considerable attention owing to its environmentally friendly and sustainable advantages.

*Trichoderma* species, well-known natural biocontrol agents capable of colonizing host plants as endophytic symbionts, are widely used to control fungal diseases due to their mycoparasitic traits [12]. Although *Trichoderma* is generally regarded as a terrestrial genus, numerous strains with biocontrol potential have been continuously isolated from mangrove plants, marine sediments, invertebrates, and macroalgae [13]. These non-terrestrial *Trichoderma* strains exhibit unique physiological traits. For instance, *Trichoderma* sp. isolated from marine environments can produce structurally diverse and novel metabolites, such as terpenoids, polyketides, peptaibols, and alkaloids, some of which display antimicrobial, cytotoxic, and anti-inflammatory activities [14,15]. In this study, we isolated an antagonistic strain of *T. harzianum*, designated as strain TH10, from marine algal sediments. Strain TH10 displayed strong antagonistic activity against *P. oryzae*. Nevertheless, *T. harzianum* TH10 powder (PTH) prepared using conventional culture techniques frequently exhibits poor agronomic performance and inconsistent biocontrol performance, limiting its practical application [16,17]. To address this problem, this study focuses on developing effective strategies to improve the agronomic performance of *T. harzianum* TH10.

Notably, root-colonizing fungi establish mutualistic symbiotic relationships by triggering root cutin or lignin biosynthesis. The degradation products of these polymers can subsequently serve as carbon sources for the fungi [18]. *T. harzianum* secretes cutinase to hydrolyze root-derived cutin, releasing C16- and C18-hydroxy fatty-acid monomers, and lignocellulases to degrade residual lignin for nutrition [19,20]. Physical contact between fungal mycelia and root cells activates plant cutin or lignin biosynthetic pathways, a response that restricts excessive fungal ingress and facilitates sustained rhizosphere colonization [21,22]. Previous studies have preliminarily revealed the cutin-dependent interaction model between *Trichoderma* and plant roots [18,23]. Given that lignocellulose resources are critical for sustaining *Trichoderma* populations in the rhizosphere, spent mushroom substrate (SMS) was considered a promising carrier for strain TH10. SMS is a by-product of edible mushroom cultivation and is rich in residual cellulose, lignin, fungal biomass, macro- and micronutrients, organic matter, and extracellular enzymes, which might facilitate the survival of strain TH10 and its rhizosphere-colonization capacity [24–26].

As mentioned above, *T. harzianum* has broad application potential in eco-friendly and sustainable biocontrol of crop diseases [27,28]. However, effective strategies for improving its rhizosphere-colonization capacity and biocontrol efficiency are still lacking [29]. This study aimed to establish an SMS-mediated strategy and explore whether SMS can improve the agronomic performance and control efficacy of strain TH10 against rice blast caused by *P. oryzae*, as well as to reveal the physiological and phenotypic characteristics associated with STH-induced growth promotion and disease resistance through greenhouse trials,

SEM, and transcriptome sequencing. Moreover, we characterized the relationships between STH-induced alterations in soil physicochemical properties and plant phytohormones. Experimentally, we demonstrated that STH promoted rice growth and improved biocontrol efficacy against rice blast. To explain these beneficial effects, we hypothesize that residual fungal mycelia in SMS act as a signal to trigger cuticular lipid accumulation in rice roots, and the resulting cuticular lipids in turn serve as abundant carbon sources for *T. harzianum*. Nevertheless, this hypothesized mechanistic causal link cannot be directly proven by the present dataset, as SMS also provides plant-available nutrients. Further functional experiments will be conducted in follow-up studies.

## 2. Materials and Methods

### *2.1. Fungal and Plant Material and Cultivation*

*T. harzianum* strain TH10 was isolated from marine algal sediments off the coast of Tianjin, Bohai Bay, China, following the isolation procedure described by Zhang et al. [30], with minor modifications. Briefly, sediment samples were aseptically collected, sealed in sterile polyethylene bags, and transported to the laboratory on ice. After serial dilution of sediment suspensions, spread-plating was carried out on potato dextrose agar (PDA, consisting of 200 g/L potato infusion, 20 g/L glucose, and 15 g/L agar, pH 6.0) supplemented with streptomycin (0.1 g/L), chloramphenicol (0.3 g/L), and rose bengal (0.02 g/L). Candidate *Trichoderma* isolates were purified by repeated streaking on fresh PDA plates and further identified by morphological and molecular characterization. Four types of SMS derived from cultivation of *Ganoderma lucidum*, *Ganoderma amboinense*, *Tricholoma matsutake*, and *Pleurotus nebrodensis* were used in this study. Samples were collected from Yuxin Edible Mushroom Planting Professional Cooperative, Yuzhou, Henan, China. The original culture medium for these edible mushrooms consisted of 79% sawdust, 20% wheat bran and 1% gypsum *w*/*w*, with the moisture content adjusted to 50–60%. Specifically, pine sawdust was used as the sole cultivation substrate for *T. matsutake*. These four SMS materials were mixed at an equal mass ratio (1:1:1:1 *w*/*w*/*w*/*w*) to obtain the mixed-SMS powder used for inoculant preparation. *P. oryzae* Guy11 used in this study was provided by Hangzhou Fengxun Biotechnology Co., Ltd. (Hangzhou, China). The strain was activated and maintained on PDA medium at 28 °C in darkness for 7 days. To harvest abundant conidia, mycelial plugs from the PDA plates were inoculated into potato dextrose broth (PDB) and incubated for 7 days at 28 °C with shaking at 180 rpm. The rice cultivar, Zhenghan 10, was used for all experiments in this study, with seeds provided by the Henan Academy of Agricultural Sciences. All strains and plant materials used in this study are listed in Table S1.

### *2.2. Preparation of SMS-Based T. harzianum Inoculants (STH)*

To obtain high-viability *T. harzianum* powder for subsequent inoculant preparation, solid-state fermentation was performed following the protocol reported by Naeimi et al., with minor modifications [31]. *T. harzianum* TH10 was first cultured and activated on PDA plates at 28 °C for 7 days. After incubation, fungal spores were eluted using sterile distilled water and diluted to a final concentration of $1 \times 10^5$ CFU/mL. The spore suspension was inoculated into sterilized substrate consisting of wheat bran and rice husk (1:1 *w*/*w*, initial pH 5.8 ± 0.2) for solid-state culture at 28 °C for 7 days, with an inoculation rate of 10% and initial substrate moisture of 50%. The fermented substrate was harvested, oven-dried at 40 °C to constant weight, milled, and passed through a 40-mesh sieve to yield spore powder [32]. Subsequently, the viable conidial concentration of TH10 spore powder was quantified via the plate-counting method. Appropriate serial dilutions of the spore powder sample were prepared, and dilutions of $10^{-6}$, $10^{-7}$, and $10^{-8}$ were spread onto PDA plates and incubated at 28 °C for 5–7 days for colony counting. Results

were expressed as $1 \times 10^{10}$ CFU/g sample. For the preparation of SMS-based TH10 (STH), four SMS materials from *Ganoderma lucidum*, *Ganoderma amboinense*, *Tricholoma matsutake*, and *Pleurotus nebrodensis* were individually ground and sieved through a 100-mesh sieve, and mixed at a mass ratio of 1:1:1:1 *w*/*w*/*w*/*w*. The initial physicochemical properties of the mixed SMS were pH 7.4, moisture content 58%, organic matter 526 g/kg, and C/N ratio 25. The pH, organic matter, and C/N ratio were within the reported ranges for raw spent mushroom substrates of various edible fungi [33]. The spore powder of TH10 was fully blended with mixed SMS powder (1:8 *w*/*w*). The mixture was humidified with sterile water, and then compressed into round tablets using a tablet press. Each tablet was 10 mm in diameter and 3 mm in thickness, with a weight of approximately 0.2 g. The viable conidial load per tablet was determined using the plate-counting method, yielding approximately $2.2 \times 10^8$ CFU per tablet. For PTH preparation, the spore powder was directly processed without the addition of SMS.

### 2.3. Activity Assessment of Strain TH10 Against Pyricularia oryzae In Vitro

*T. harzianum* TH10 and *P. oryzae* Guy11 were activated on PDA at 28 °C in darkness for 7 d. Six-mm mycelial plugs of each fungus were placed 3 cm apart on opposite sides of fresh PDA plates and incubated under identical conditions for dual-culture interaction observation. Agar blocks of around 1 $cm^2$ were excised from single-culture plates of each strain and the interaction zone of confrontation plates, air-dried and gold-sputtered. The samples were subsequently observed with a ZEISS MERLIN compact scanning electron microscope (SEM) (Zeiss, Jena, Germany) for qualitative observation of morphological changes in Guy11 hyphae and the antagonistic interaction between strain TH10 and Guy11. The antifungal activity of extracellular secretions produced by strain TH10 against *P. oryzae* Guy11 was determined by a mycelial inhibition assay. The broth of strain TH10, cultured in PDB at 28 °C and 180 rpm for 7 d (viable population: $2.4 \times 10^9$ CFU/mL), was centrifuged, and the resulting supernatant was sterilized by filtration through a 0.22 μm membrane to obtain a cell-free filtrate for subsequent antifungal assays.

The cell-free filtrate was serially diluted 10-fold from $\times 10^{-1}$ to $\times 10^{-7}$, and 200 μL of each diluted filtrate was spread evenly onto a PDA plate. Once the plate surface dried naturally, a 6 mm mycelial plug of Guy11 was inoculated at the plate center. After incubation at 28 °C in darkness for 7 d, Guy11 colony diameters were measured by the cross-diameter method to calculate the inhibition rate according to Formula (1):

$$\mu(\%) = \frac{D_{ck} - D_x}{D_{ck} - D_0} \times 100 \quad (1)$$

where $\mu$ stands for the mycelial inhibition rate, $D_{CK}$ represents the colony diameter of the blank control group, $D_X$ denotes the colony diameter of the treatment group, and $D_0$ is the initial diameter of the inoculated mycelial plug. Linear regression was performed with inhibition rate on the Y-axis and the logarithm of the dilution factor on the X-axis. The fitted regression equation was used to calculate the $EC_{50}$ value of strain TH10 against *P. oryzae* Guy11. All activity assays were performed in triplicate.

### 2.4. Rice Blast Disease Model Establishment and Biocontrol Evaluation

Healthy, disease-free rice seeds were selected and surface-sterilized by soaking in 75% $C_2H_5OH$ for 30 s with vigorous shaking, followed by immersion in 1% NaClO solution for 8–10 min with repeated inverting. After rinsing with sterile water five times, the seeds were soaked in the same water and germinated at 28 °C in darkness for 72 h. Germinated seeds were sown in seedling trays and cultivated to the three-leaf stage. Seedlings of uniform growth were then transplanted into plastic pots. Each pot contained 5.0 kg of

air-dried paddy soil collected from local paddy field (Xuchang, Henan Province, China), and served as one independent biological replicate. Each pot had six planting hills, with six rice seedlings transplanted per hill. For STH treatment, 5 tablets (total 1 g) were applied per planting hole, containing $1.10 \times 10^9$ CFU viable TH10 conidia; for PTH treatment, 0.11 g inoculant ($1.10 \times 10^9$ CFU) was used per hole to achieve equivalent conidial dosage. The mixed SMS addition corresponded to 1.067 g of mixed SMS per kg soil, applied to a soil depth of approximately 2–3 cm around rice seedling roots prior to transplanting. Three independent pots were established per treatment. The rice seedlings receiving no inoculant treatment served as the control (CK). The experiment used a randomized complete-block design (RCBD) with three replicates. Seven treatments were tested: PTH, STH, *G. lucidum* SMS-based TH10, *T. matsutake* SMS-based TH10, *P. nebrodensis* SMS-based TH10, *G. amboinense* SMS-based TH10, and an untreated control (CK). One pot served as one replicate. The RCBD experimental layout is shown in Figure S1; each row represented one block containing all seven treatments, and pots within each block were randomly arranged under greenhouse conditions. Data obtained from this greenhouse RCBD trial were analyzed by one-way ANOVA, and mean separations were performed using Duncan's multiple-range test at $p < 0.05$. Due to space limitations, an SMS-only treatment was not included, and therefore the individual effects of SMS and TH10 cannot be fully separated in the present study.

A detached leaf inoculation assay was conducted to evaluate the biocontrol potential of strain TH10 against rice blast. Healthy rice leaves were collected from the above potted rice seedlings at the early tillering stage, surface-sterilized, and placed on moist filter paper for the detached-leaf assay. The conidial suspension of *P. oryzae* Guy11 ($1 \times 10^5$ CFU/mL) was used for inoculation by dropping it onto the wound sites. Inoculated leaves were incubated at 28 °C with relative humidity > 90% under a 12 h light/12 h dark photoperiod, and strain TH10 cell-free supernatant was sprayed onto inoculation sites every other day. Each treatment contained six biological replicates, with sterile water treatment (CK1) and single *P. oryzae* inoculation (CK2) as controls. Lesion development was monitored at 2, 4, and 6 dpi. Lesion length and width were measured to assess disease severity, and the cross-diameter method was applied to calculate equivalent lesion diameters. For sequential lesion-size measurements obtained from the same detached leaves at 2, 4, and 6 dpi, repeated-measures ANOVA was performed to assess the effects of treatment, time, and their treatment-by-time interaction. Leaf blast was surveyed at 7, 14 and 21 days post *P. oryzae* inoculation. Leaf blast severity was evaluated according to the 0–9 Standard Evaluation System (SES) scale standard of the International Rice Research Institute (IRRI, 2013) [32]. The lesion expansion rate was calculated using the following Formula (2):

$$\text{Lesion expansion rate } (\%) = \left(\frac{D_{6\text{dpi}} - D_{2\text{dpi}}}{D_{2\text{dpi}}}\right) \times 100 \quad (2)$$

where $D_{2\text{dpi}}$ and $D_{6\text{dpi}}$ represent the equivalent lesion diameters at 2 dpi and 6 dpi, respectively.

At the tillering stage, the nodal tissues were inoculated with *P. oryzae* Guy11 using a modified toothpick-inoculation method from Kumar et al. [34]. Briefly, sterile toothpicks were used to prick actively growing Guy11 mycelial mats on PDA plates to harvest fresh mycelium, followed by piercing rice internode tissues for inoculation. After inoculation, the relative humidity was maintained at >90%, and the plants were incubated at 28 °C. At maturity, one hill consisting of six seedlings was sampled from each independent pot for panicle-blast severity assessment. Panicle-blast severity was calculated as the percentage of withered spikelets relative to total spikelets per panicle. Disease grades were

evaluated according to the Standard Evaluation System for Rice Panicle-blast severity (%) was calculated using the following Formula (3):

$$\text{Panicle-blast severity } (\%) = \frac{\text{Withered spikelets per panicle}}{\text{Total spikelets per panicle}} \times 100 \quad (3)$$

### *2.5. Vegetative Growth and Biological Characteristics Assessment*

To assess vegetative growth, six plants were randomly selected from each pot to determine rice plant height, root length, and above- and below-ground dry weights at the three-leaf, tillering, and jointing stages. Plants within each pot were pooled, and pot-averaged values were used for subsequent statistical analysis. The panicles were air-dried in a cool, dry place, and their moisture content was monitored using an SF101 coulometric Karl-Fischer analyzer (Shandong SF Analytical Instrument Co., Ltd., Zibo, Shandong, China) until it dropped below 13.5%, and then manually threshed for yield-component analysis. The number of grains per panicle and seed-setting rate were recorded. One hundred plump grains were randomly selected and weighed to calculate the 1000-grain weight according to Formula (4),

$$W_{1000} = \overline{W_{100}} \times 10 \quad (4)$$

where $W_{1000}$ is the 1000-grain weight (g), and $\overline{W_{100}}$ represents the average weight of 100 plump rice grains (g). All measurements were performed in triplicate using independent pots. Theoretical yield was further calculated based on yield components.

### *2.6. Observation of Rice Root Tissue*

Rice root tissue was observed under a ZEISS MERLIN compact scanning electron microscope (SEM) (Zeiss, Jena, Germany). At 14 days after STH and PTH treatment, 0.5–1.0 cm root-tip segments collected from each pot were cut into 5 mm pieces and longitudinally dissected. After washing three times using double-distilled water, the samples were fixed in 2.5% glutaraldehyde at 4 °C overnight, rinsed three times with 0.1 M phosphate-buffered saline (PBS) for 15 min each, and dehydrated through a graded ethanol series of 30%, 50%, 70%, 80%, 90%, and 100% (twice), with each step lasting 15–20 min. After vacuum freeze-drying, the samples were coated with an ETD 2000C ion coater (Beijing Elaborate Technology, Beijing, China) and observed under SEM to provide qualitative morphological evidence for fungal hyphae on rice roots. Roots without any treatment were used as the control (CK).

### *2.7. Rhizosphere Soil Physicochemical Properties (RSPP) Determination*

The initial alkaline paddy soil had a pH of 7.51, and no additional chemical fertilizers were used in this greenhouse experiment. Four types of SMS, including *Ganoderma lucidum*, *Tricholoma matsutake*, *Pleurotus nebrodensis* and *Ganoderma amboinense*, were separately used to prepare STHs, which were applied at 1 g per planting hole into pots holding 5.0 kg paddy soil by hole placement before rice transplanting. An SMS-only treatment was included, where four types of SMS powder without strain TH10 were applied at the same dosage of 1 g per planting hole, to separate the effects originating from SMS itself. Soil from untreated-control pots represented the experimental baseline soil condition. Rhizosphere soil samples were collected from each treatment pot at the tillering stage, retaining only soil tightly attached to root surfaces after shaking off loose bulk soil, and air-dried for physicochemical analysis. RSPP were determined with reference to official recommended forestry industry standards [35]. Soil total nitrogen (TN) was determined by the Kjeldahl digestion-distillation titration method, and alkaline-hydrolyzable nitrogen (AN) was detected using the alkaline diffusion method according to LY/T 1228-2015. Soil total phos-

phorus (TP) and available phosphorus (AP) were analyzed by the molybdenum-antimony anti-spectrophotometric method following LY/T 1232-2015. Soil total potassium (TK) and rapidly available potassium (AK) were measured by flame photometry in accordance with LY/T 1234-2015. Soil organic matter (OM) was determined by the potassium dichromate oil-bath heating titration method as specified in NY/T 1121.6-2006. Soil pH was tested using potentiometry with a water–soil ratio of 2.5:1, according to HJ 962-2018. The experiment was conducted with self-prepared reagents instead of commercial test kits and arranged in a randomized complete-block design with three replicates. However, these SMS-only pots were not incorporated into the greenhouse biological assay owing to space limitations. As a result, we cannot completely separate the effects of SMS and TH10.

### *2.8. Transcriptome Sequencing and Analysis*

Samples were collected at the jointing stage from leaves and roots of rice plants in the STH and PTH treatment and control groups. The samples were immediately frozen in liquid nitrogen and stored at −80 °C. Total RNA was extracted using the MJZol Total RNA Extraction Kit (Shanghai Meiji Junhua Biomedical Technology Co., Ltd., Shanghai, China). RNA concentration and purity were assessed using a Nanodrop 2000 spectrophotometer (Thermo Fisher Scientific, Wilmington, DE, USA), and RNA integrity was verified by agarose gel electrophoresis; samples with $RIN \geq 7.0$ were considered qualified. Qualified RNA samples were used to construct strand-specific libraries and sequenced on the Illumina NovaSeq X Plus platform (Illumina Inc., San Diego, CA, USA) with 150 bp paired-end reads. Raw reads were quality-filtered using fastp, and the resulting clean reads were aligned to the rice reference genome (MSU 7.0) using Hisat2, followed by quantification of gene expression levels. Differential expression analysis was performed using DESeq2, with significance thresholds set at $p < 0.05$ and $|\log_2 FC| \geq 1.0$. GO and KEGG enrichment analyses were conducted on the differentially expressed genes. All transcriptome-sequencing analyses were performed in triplicate.

### *2.9. Determination of SA, ABA, and GA3 Content*

Endogenous gibberellin ($GA_3$), abscisic acid (ABA), and salicylic acid (SA) contents in rice plants were determined using high-performance liquid chromatography (HPLC). Fresh plant samples (0.2 g) were ground in liquid nitrogen and extracted with 750 µL of extraction solution (methanol:ultrapure water:glacial acetic acid = 80:19:1, $v/v/v$) at 4 °C on a rotary shaker at 300 rpm overnight. After centrifugation at 10,000 rpm for 20 min at 4 °C, the supernatant was collected. The pellet was re-extracted with 450 µL of the same extraction solution at 4 °C on a rotary shaker at 300 rpm for 4 h, and centrifuged at 10,000 rpm for 20 min at 4 °C. The two supernatants were combined, filtered through a 0.22 µm membrane, mixed with 300 µL of 0.1% formic acid, and centrifuged at 10,000 rpm for 15 min at 4 °C to obtain the final sample solution.

Chromatographic separation was performed on an ACCHROM XAqua C18 column (4.6 × 250 mm, 5 µm), Acchrom Technologies Co., Ltd., Beijing, China, at 40 °C. The mobile phase consisted of 0.1% formic acid in water (A) and methanol (B) under isocratic elution at a flow rate of 1.0 mL/min, with an injection volume of 10 µL. The detection wavelengths were set at 210 nm and 254 nm with full wavelength scanning. Standard curves were constructed using serial dilutions of authentic standards, with a linear range of 0.125–4 mg/L, which fully covered the hormone concentration range (0.2–3 mg/L) detected in the samples. Each endogenous phytohormone was measured in triplicate.

### *2.10. Statistical Analysis*

All experiments were performed with at least three biological replicates. Plant-growth-related indices including shoot height, root length and biomass were determined via

destructive sampling at individual developmental stages; different batches of experimental units were used for each time-point measurement. A separate one-way ANOVA was therefore applied to data from each developmental stage. All statistical analyses were performed using R 4.5.2 software. One-way analysis of variance (ANOVA) was conducted for phenotypic disease parameters, physiological indexes, phytohormone contents, and in vitro antagonism test data. Significant differences between group means were determined by Duncan's multiple-range test at $p < 0.05$. For multiple soil physicochemical variables evaluated within the same experiment, no formal correction for multiple testing was applied; results are interpreted with caution and presented for descriptive purposes. The dose–response regression used to calculate the $EC_{50}$ value of strain TH10 cell-free culture filtrate was performed in Origin 2019b. All experimental data were expressed as means ± standard deviation (SD). Clean reads obtained after quality control of transcriptome sequencing data were aligned to the rice reference genome using HISAT2. Gene expression abundance was quantified with RSEM. Differentially expressed genes (DEGs) were screened using the embedded DESeq2 module on the Majorbio cloud-based platform (https://www.majorbio.com/), with thresholds of $|\log_2(\text{fold change})| \geq 1.0$ and adjusted $p$-value < 0.05. DESeq2 implements Benjamini–Hochberg correction for multiple testing for transcriptomic DEG identification. KEGG enrichment analyses for transcriptomic datasets were also conducted on the Majorbio cloud-based platform.

## 3. Results

### *3.1. In Vitro Antagonistic Activity of Trichoderma harzianum TH10 Against Pyricularia oryzae*

#### 3.1.1. Preliminary Antagonism Identification of Strain TH10 Against *P. oryzae* Guy11

To preliminarily verify the antifungal potential of strain TH10 against *P. oryzae* Guy11, we used dual-culture assays and scanning electron microscopy (SEM) observations to investigate its antagonistic behaviors and systematically characterize its antagonistic modes of action (MOA) [36]. The phenotypes on confrontation plates were sequentially recorded at 3, 7, and 14 days post-inoculation (dpi) and displayed in Figure 1a. On day 3, a distinct and well-defined inhibition zone appeared around Guy11 colonies, demonstrating that strain TH10 secreted antagonistic metabolites to inhibit the mycelial growth of Guy11 by inducing mycelial lysis. With incubation prolonged for 7 days, the mycelia of strain TH10 gradually spread towards the interaction zone and partially colonized this area. The original inhibition zone faded gradually, and abundant conidia began to form. At 14 dpi, strain TH10 covered the whole plate and bore abundant green conidia, rendering the colony green. The radial-direction growth of Guy11 hyphae was significantly suppressed, and no mycelial interweaving was observed between the two strains, indicating strong spatial-site competition.

Mycelial samples collected from the dual-culture interaction zone were observed by SEM to investigate hyphal interactions. The three SEM images in Figure 1b from left to right represent monocultured Guy11 hyphae, the hyphal contact interface of Guy11 and strain TH10, and monocultured strain TH10 hyphae. These micrographs revealed that abundant hyphae of strain TH10 tightly adhered to, twisted around, and fully encased the hyphae and conidia of Guy11. Such heavy encapsulation caused severe morphological deformation of vegetative and reproductive structures in Guy11 and inhibited the formation of mature conidia. In contrast, the Guy11 strain grown in monoculture produced intact, well-differentiated, plump and uniform hyphae and conidia. The slight shrinkage and distortion of Guy11 cell walls were presumably induced by metabolites secreted by strain TH10.

Taken together, macroscopic and microscopic phenotypic observations suggested that strain TH10 inhibits Guy11 through three distinct antagonistic MOAs, including metabolite-mediated long-distance inhibition, spatial exclusion, and direct mycoparasitism accompanied by the coiling and degradation of pathogen hyphae and conidia. The three antagonistic MOAs

exert synergistic effects to suppress the proliferation of Guy11, simultaneously inhibiting colony expansion and disrupting its cellular morphological development.

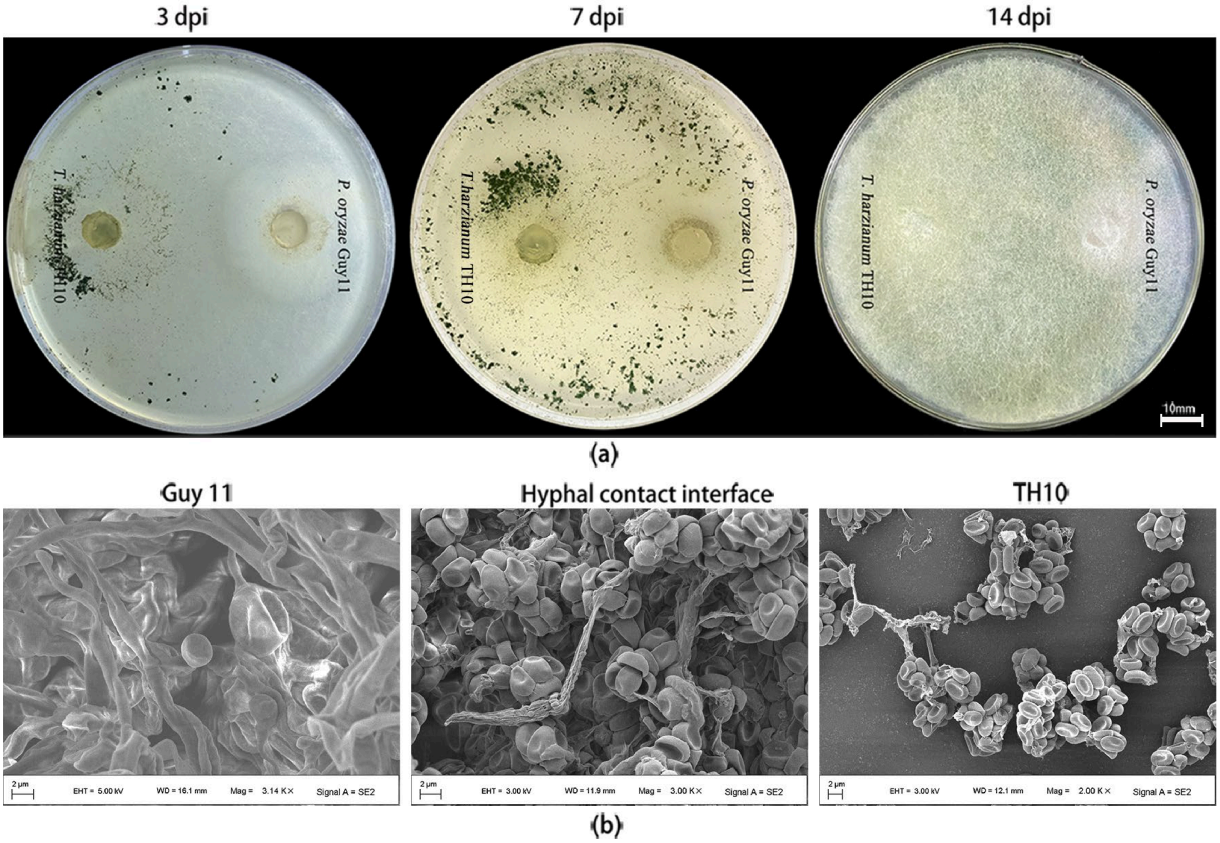



**Figure 1.** Antagonistic activity of strain TH10 against *P. oryzae* Guy11. (**a**) Time-course dual-culture assay of *T. harzianum* TH10 and Guy11 at 3, 7, and 14 dpi. Each plate was inoculated with *T. harzianum* TH10 on the left and *P. oryzae* Guy11 on the right. Scale bar: 10 mm; (**b**) SEM images arranged from left to right: monocultured Guy11, hyphal contact interface, and monocultured strain TH10. Scale bar: 2 μm.

### 3.1.2. Antifungal Activity of Strain TH10 Secretions Against *P. oryzae* Guy11

Previous studies have reported that *Trichoderma* strains can secrete trichotoxins and diverse bioactive metabolites to suppress the growth of phytopathogens [37]. To further confirm that the extracellular metabolites secreted by strain TH10 exert antifungal activity against *P. oryzae* Guy11, gradient-dilution assays were performed to determine the half-maximal effective concentration ($EC_{50}$) of its cell-free supernatant [38]. Serial ten-fold dilutions ranging from $\times 10^{-1}$ to $\times 10^{-7}$ were prepared for antifungal testing. Each diluted filtrate was evenly spread onto PDA plates. Mycelial plugs of Guy11 were subsequently inoculated onto the metabolite-treated plates, followed by incubation at 28 °C to observe mycelial growth. Results showed that the supernatant had a significant inhibitory effect on the mycelial growth of Guy11 in a concentration-dependent manner, and higher supernatant concentrations led to stronger inhibition of radial mycelial growth. As shown in Figure S2, the highest inhibition rate of 70.00% was observed under the 10-fold dilution treatment. Antifungal activity dropped progressively with increasing dilution factor, with a 21.33% inhibition rate remaining at the $10^5$-fold dilution.

The cross-diameter method was employed to measure the colony diameters of Guy11. The mycelial-growth inhibition rates were subsequently calculated to determine the $EC_{50}$ value. $EC_{50}$ was calculated by fitting the dose–response regression equation, which was $\mu = -14.15 \log_{10}(n) + 93.88$ ($R^2 = 0.9942$). Here, $n$ represents the dilution factor of the

original fermentation filtrate, $\mu$ stands for the mycelial inhibition rate (%), and $R^2$ denotes the coefficient of determination. Accordingly, the corresponding $EC_{50}$ value was determined to be a $1.262 \times 10^3$-fold dilution of the original filtrate. These quantitative data were highly consistent with the macroscopic antagonism phenotype, including well-defined inhibition zones observed during dual-culture testing, which indicated that strain TH10 suppresses the mycelial growth of Guy11 by secreting extracellular bioactive metabolites (Supplementary Data S1).

### *3.2. Assessment of SMS-Based TH10 for Rice Blast Biocontrol and Rice Growth Promotion*

#### 3.2.1. Strain TH10 Biocontrol of Rice Blast

The dual-culture assays confirmed that strain TH10 exerted significant inhibitory effects on *P. oryzae* Guy11. Accordingly, detached rice-leaf inoculation assays were performed to further evaluate the biocontrol potential of *T. harzianum* TH10 against rice blast. The cell-free culture supernatant of strain TH10 was sprayed onto the inoculation site of Guy11 on detached rice leaves every other day. Six biological replicates were arranged for each treatment. The mechanical-wound group (CK1) and the Guy11-inoculated group (CK2), each sprayed with sterile water, served as controls. Lesion progression was recorded at 2, 4, and 6 dpi, and the results are shown in Figure 2a. Lesion length and width were measured to determine disease severity, and the cross-diameter method was used to calculate the equivalent lesion diameter, and all quantitative results are displayed in Figure 2b and Table S2.

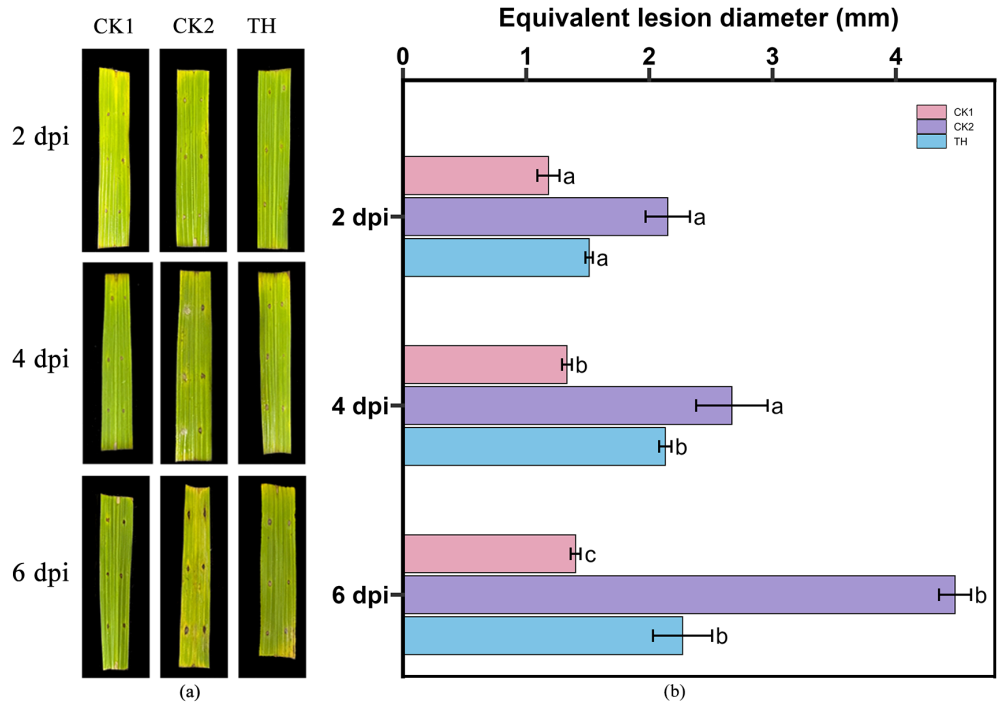



**Figure 2.** Biocontrol assessment of strain TH10 against rice blast. (**a**) Detached leaf blast symptoms at 2, 4 and 6 dpi. Scale bar = 2 mm. (**b**) Temporal quantitative analysis of lesion equivalent-diameter ($n = 6$). Different lowercase letters denote significant differences at $p < 0.05$. CK1: mechanical-wound group sprayed with sterile water; CK2: Guy11-inoculated group sprayed with sterile water; TH: Guy11-inoculated group sprayed with strain TH10 cell-free culture supernatant.

Faint physiological brown speckles appeared on rice leaves treated with sterile water (CK1). The speckle diameter reached $1.18 \pm 0.09$ mm on day 2 and $1.40 \pm 0.04$ mm on day 6, corresponding to an expansion of approximately 18.64%, while the disease grade remained 0. In contrast, lesions expanded significantly on leaves inoculated with Guy11 alone (CK2). The lesion diameter reached $2.15 \pm 0.18$ mm at 2 dpi and $4.48 \pm 0.13$ mm at 6 dpi,

corresponding to an expansion of approximately 108.37%, with the disease grade reaching 6. However, leaf-blast symptoms were markedly suppressed after spraying the strain TH10 supernatant onto Guy11-inoculated sites. Compared with the value measured at 2 dpi, the lesion diameter increased by approximately 50.33% at 6 dpi, which corresponded to a disease grade of 3. Detached rice-leaf assays revealed that strain TH10 exhibited strong inhibitory activity against *P. oryzae* Guy11. We subsequently performed greenhouse pot trials to evaluate the biocontrol efficacy of PTH and STH, in which rice blast was triggered by inoculating rice tiller nodes with Guy11 mycelia.

At maturity, panicle blast severity was assessed according to the Standard Evaluation System for Rice. Rice panicles and the potted-plant growth status under the three treatments are presented in Figure S3. Raw spikelet count data used to calculate panicle blast severity and biocontrol efficacy are provided in Table S3. This metric reflects disease severity rather than classical disease incidence. Data in Table 1 reveal that the STH treatment significantly reduced disease severity to 14.60 ± 2.68%, with a greenhouse biocontrol efficacy of 51.34 ± 6.39% and a 51.89% inhibition rate of withered grains. The plants showed a moderately susceptible disease grade of 3. In contrast, PTH treatment reduced disease severity to 25.94 ± 2.75%, with a greenhouse biocontrol efficacy of 12.56 ± 18.81% and a panicle-blast severity inhibition rate of 14.53%, which was classified as disease grade 5. The large standard deviation indicated unstable biocontrol efficacy of PTH among greenhouse experimental replicates. The in planta assay showed that both treatments effectively alleviated panicle-blast damage, and STH showed a superior disease-suppressive effect compared with PTH. By comparison, the untreated control group (CK) exhibited a panicle-blast severity of 30.35 ± 5.94%, which attained the highly susceptible disease grade 7. The mitigation of panicle-blast damage further affected grain yield performance, so the seed-setting rate was highest for STH, followed by PTH and then the untreated control, with values of 85.40 ± 2.68%, 74.06 ± 2.75%, and 69.65 ± 5.94%, respectively.

**Table 1.** Effects of SMS-based *T. harzianum* TH10 on rice blast resistance.

| | Panicle Blast | | Panicle-Blast Severity Inhibition Rate (%) | Seed-Setting Rate (%) |
|---|---|---|---|---|
| | Disease Severity (%) | Greenhouse Biocontrol Efficacy (%) | | |
| CK | 30.35 ± 5.94 [a] | n.d. | 0.00 | 69.65 ± 5.94 [a] |
| PTH | 25.94 ± 2.75 [ab] | 12.56 ± 18.81 | 14.53 | 74.06 ± 2.75 [a] |
| STH | 14.60 ± 2.68 [c] | 51.34 ± 6.39 | 51.89 | 85.40 ± 2.68 [b] |

Data are presented as mean ± SD of three independent experimental pots. One hill (six plants per hill) was sampled from each pot as a subsample. Different lowercase letters denote significant differences among Guy11-inoculated CK, PTH and STH treatments ($p < 0.05$). n.d., not detected. CK: untreated-control plants; PTH: plants hole-applied with strain TH10 powder; STH: plants hole-applied with SMS-based TH10 inoculant. *Panicle-blast severity* (%) = *Withered spikelets per panicle*/*Total spikelets per panicle* × 100. Seed-setting rate (%) = 1 − panicle-blast severity.

#### 3.2.2. SMS-Mediated Rice Growth Promotion by Strain TH10

Concurrently with the greenhouse experiment, rice growth traits were determined at different vegetative stages to compare the growth-regulating effects of STH and PTH. As shown in Table 2, when treated with STH, rice reached a plant height of 14.29 ± 2.94 cm at the three-leaf stage, which exceeded that under PTH treatment by 0.56% and that of untreated seedlings by 2.22%. At the tillering stage, the plant height of rice under STH treatment was 26.48% and 51.77% higher than that of the PTH group and the untreated-control seedlings, respectively. The corresponding promotion values stood at 19.53% and 44.97% at the jointing stage. Consistent trends were also observed for root length, shoot dry weight, and root dry weight at all developmental stages. Compared with PTH and CK, the STH treatment

increased root length by 25.02–29.51% and 60–75%, root dry weight by 40–45% and 70–80%, and shoot dry weight by 3–4% and 7–8%, respectively. Furthermore, the dynamics of tiller development revealed that STH exhibited stronger promoting effects on tiller initiation and emergence at the mid-to-late tillering stage, producing a maximum net tiller increment of 17 and the highest relative growth rate of 54.84%, the latter being 23.13% and 3.23% higher than those of the untreated-control and PTH-treated groups, respectively. Finally, the STH-treated rice exhibited the most vigorous vegetative growth, with its 1000-grain weight reaching 26.10 ± 0.46 g, 23.70% and 12.99% higher than those of the untreated control and PTH-treated groups, respectively. The observed growth-promoting effects cannot be solely attributed to *T. harzianum* TH10, since SMS itself supplies organic matter and nutrients. Collectively, strain TH10 carried by SMS may contribute to promoted root elongation and below-ground biomass accumulation, which in turn improved water and nutrient uptake, enhanced above-ground biomass production and sustained tiller emergence.

### *3.3. Analysis on the Biocontrol Mechanism of SMS-Based TH10 Strain*

#### 3.3.1. SMS-Mediated Effects of Strain TH10 on Rhizosphere Soil

Greenhouse pot trials demonstrated that STH treatments exerted growth-promoting effects on rice. To further elucidate the causes behind this phenomenon, samples of rhizosphere soil tightly attached to rice roots from all treatments were collected at the rice tillering stage for physicochemical analysis. Soil from untreated-control pots served as the baseline soil condition for this experiment, with additional SMS-only groups set to distinguish the effects of SMS itself from SMS + TH10 treatments. In this experiment, nine soil physicochemical indicators were determined to evaluate rhizosphere-soil improvement across four SMS-based TH10 treatments, with substrates obtained from *Ganoderma lucidum*, *Tricholoma matsutake*, *Pleurotus nebrodensis* and *Ganoderma amboinense*. The detected indices included total nitrogen (TN), total phosphorus (TP), total potassium (TK), total salt (TS), alkali-hydrolyzable nitrogen (AN), available phosphorus (AP), available potassium (AK), organic matter (OM) and soil pH. Differences in rhizosphere soil properties among different STH treatments are shown in Figure 3. For soil TN, Figure 3a shows that SMS-based TH10 strains significantly increased soil TN compared with the untreated control, with the STH derived from *G. amboinense* producing the largest increase in TN (7.847 ± 0.587 g·kg$^{-1}$, $p < 0.01$). With respect to TP content, Figure 3b shows that STH markedly enhanced phosphorus accumulation, and the highest TP concentration was detected under the *G. amboinense* STH treatment (1.632 ± 0.138 g·kg$^{-1}$, $p < 0.01$). As presented in Figure 3c, TK concentrations in all STH-inoculated treatments were significantly lower than those of the untreated control, with the greatest reduction in TK observed under the *T. matsutake* STH treatment (12.517 ± 0.144 g·kg$^{-1}$, $p < 0.01$). For soil TS, Figure 3d shows that all treatments, except the *P. nebrodensis* STH group, exhibited extremely significant differences compared with the untreated control. The STH derived from *G. amboinense* produced the greatest reduction in soil salinity (0.164 ± 0.034%, $p < 0.001$). Turning to AN, Figure 3e indicates that AN was substantially enhanced after STH addition, and application of *T. matsutake* STH achieved the highest AN concentration (979.377 ± 90.491 mg·kg$^{-1}$, $p < 0.01$). In terms of AP, Figure 3f illustrates that all STH amendments resulted in significantly higher AP levels compared with untreated soil, and application of *G. amboinense* STH exhibited the largest AP accumulation (448.522 ± 26.919 mg·kg$^{-1}$, $p < 0.01$). For soil AK, Figure 3g shows that STH application significantly improved soil available potassium status, and the most prominent AK increase was found with application of *P. nebrodensis* STH (2.305 ± 0.252 g·kg$^{-1}$, $p < 0.01$). With respect to OM, Figure 3h demonstrates that OM content was significantly enriched by STH incorporation, and application of *G. lucidum* STH yielded the highest OM concentration (139.524 ± 10.007 g·kg$^{-1}$, $p < 0.01$). For soil pH, Figure 3i shows that only *P. nebrodensis* SMS treatment significantly decreased rhizosphere soil pH, while the other three single SMS treatments and CK maintained moderately alkaline soil pH.

**Table 2.** Effects of SMS-based *T. harzianum* TH10 on biological characteristics of rice.

| Biological Characteristics | Three-Leaf Stage | | | Tillering Stage | | | Jointing Stage | | | Maturity Stage | | |
|---|---|---|---|---|---|---|---|---|---|---|---|---|
| | CK | PTH | STH | CK | PTH | STH | CK | PTH | STH | CK | PTH | STH |
| Plant height/cm | 13.98 ± 2.24 $^{a}$ | 14.21 ± 2.55 $^{a}$ | 14.29 ± 2.94 $^{a}$ | 20.96 ± 1.42 $^{a}$ | 25.15 ± 2.66 $^{b}$ | 31.81 ± 3.19 $^{c}$ | 29.51 ± 2.52 $^{a}$ | 35.79 ± 1.19 $^{b}$ | 42.78 ± 2.07 $^{c}$ | 82.37 ± 0.71 $^{c}$ | 99.88 ± 1.26 $^{b}$ | 103.30 ± 0.51 $^{a}$ |
| Root length/cm | 5.93 ± 0.92 $^{a}$ | 7.93 ± 0.35 $^{b}$ | 10.27 ± 0.45 $^{c}$ | 10.32 ± 0.42 $^{a}$ | 14.27 ± 0.54 $^{b}$ | 17.83 ± 0.44 $^{c}$ | 17.69 ± 1.04 $^{a}$ | 22.58 ± 0.78 $^{b}$ | 28.23 ± 0.56 $^{c}$ | 23.20 ± 0.56 $^{a}$ | 26.08 ± 0.76 $^{b}$ | 30.22 ± 0.46 $^{c}$ |
| Shoot dry weight/g | 1.08 ± 0.05 $^{b}$ | 1.11 ± 0.02 $^{ab}$ | 1.15 ± 0.06 $^{b}$ | 1.72 ± 0.03 $^{a}$ | 1.79 ± 0.02 $^{b}$ | 1.85 ± 0.06 $^{c}$ | 2.31 ± 0.05 $^{a}$ | 2.45 ± 0.04 $^{b}$ | 2.53 ± 0.07 $^{c}$ | 10.17 ± 0.38 $^{a}$ | 10.99 ± 0.38 $^{b}$ | 11.87 ± 0.21 $^{c}$ |
| Root dry weight/g | 0.45 ± 0.03 $^{c}$ | 0.52 ± 0.03 $^{b}$ | 0.56 ± 0.04 $^{a}$ | 0.53 ± 0.03 $^{c}$ | 0.65 ± 0.05 $^{b}$ | 0.93 ± 0.03 $^{a}$ | 0.77 ± 0.05 $^{c}$ | 0.86 ± 0.07 $^{b}$ | 1.19 ± 0.06 $^{a}$ | 3.65 ± 0.35 $^{c}$ | 4.55 ± 0.27 $^{b}$ | 5.31 ± 0.34 $^{a}$ |
| Net tiller increase per pot | n.d. | n.d. | n.d. | 13 | 16 | 17 | n.d. | n.d. | n.d. | n.d. | n.d. | n.d. |
| 1000-grain weight/g | n.d. | n.d. | n.d. | n.d. | n.d. | n.d. | n.d. | n.d. | n.d. | 21.10 ± 0.20 $^{c}$ | 23.10 ± 0.30 $^{b}$ | 26.10 ± 0.46 $^{a}$ |

Data in the table are expressed as mean ± SD ($n$ = 3), where $n$ represents three independent experimental pots. Six randomly selected plants were sampled from each pot for measurement. CK, PTH and STH refer to the untreated control, powdered strain TH10 and SMS-based TH10 groups exposed to Guy11-induced blast stress, respectively. Different lowercase letters indicate significant differences among treatments within the same growth stage at $p < 0.05$ based on Duncan's multiple-range test; identical letters indicate no significant difference. n.d., not determined.

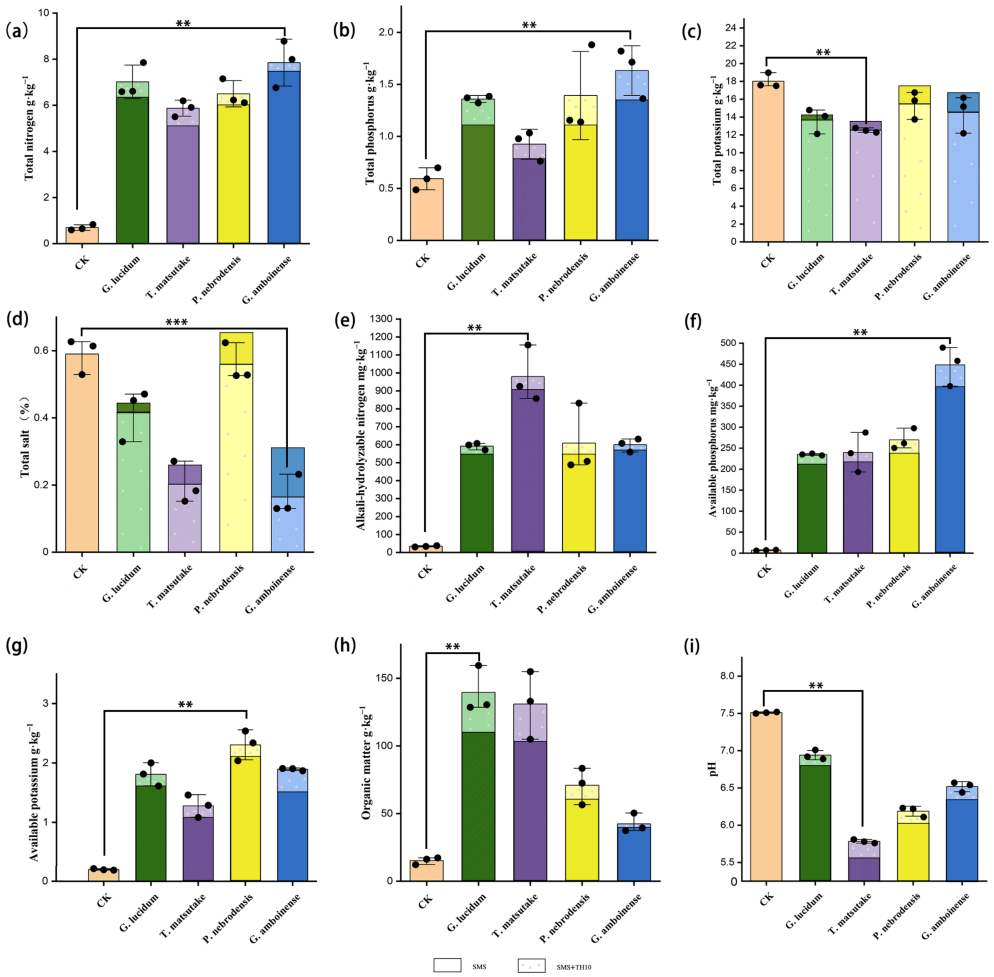



**Figure 3.** Determination of soil physicochemical properties with different STH treatments. (**a**) The content of total nitrogen; (**b**) The content of total phosphorus; (**c**) The content of total potassium; (**d**) The content of total salt; (**e**) The content of alkali-hydrolyzable nitrogen; (**f**) The content of available phosphorus; (**g**) The content of available potassium; (**h**) The content of organic matter; (**i**) Soil pH value. CK: untreated-control soil; *G. lucidum*: treated with *G. lucidum* STH; *T. matsutake*: treated with *T. matsutake* STH; *P. nebrodensis*: treated with *P. nebrodensis* STH; *G. amboinense*: treated with *G. amboinense* STH. Bars with white triangular patterns represent SMS + TH10 treatments, while solid shaded bars denote SMS-only treatments. Asterisks denote significant differences relative to CK (** $p < 0.01$, *** $p < 0.001$). Error bars indicate S.D. ($n = 3$).

The above results indicated that compared with untreated soil, most SMS-based TH10 treatments significantly elevated TN, TP, AN, AP, AK and OM, while reducing both TK and TS. Compared with the control, the *G. lucidum* STH and *T. matsutake* STH treatments had significantly lowered total potassium concentrations but an obvious rise in available potassium. Compared with SMS-only treatments, SMS + TH10 treatments induced greater alterations in most soil physicochemical indicators. In addition, these changes in total salt may alleviate root-associated salt stress and modify soil nutrient bioavailability (Supplementary Data S2).

### 3.3.2. Comparison of Strain TH10 Colonization in Root Tissues

At the tillering stage, we found the total root length under STH treatment was 72.77% more than that of untreated root, and 24.95% higher than that of PTH treatment. The untreated roots displayed sparse root branching and the lowest root biomass. Application of PTH slightly stimulated taproot elongation, but inhibited the development of lateral and fibrous roots. In contrast, the STH treatment substantially triggered abundant proliferation

of lateral and fibrous roots, resulting in a highly branched root system. Its root length reached 17.83 ± 0.44 cm and root dry weight reached 0.93 ± 0.03 g, which were increased by 43.08% and 75.47% relative to PTH and CK, respectively, as shown in Figure 4a. To further reveal the differences in rice root growth and root architecture, the overall surface morphology and internal structure of longitudinal root sections were observed using SEM. The results shown in Figure 4b revealed distinct differences in root surface morphology among all groups. Specifically, the STH-treated rice roots exhibited extensive hyphal colonization on the root epidermis, with dense intertwined hyphal networks. In contrast, hyphae loosely adhered to the root epidermis in the PTH-treated group, resulting in low hyphal coverage on the root surface. By comparison, no hyphae were detected on untreated-control roots, which exhibited smooth and intact epidermis. Observations of longitudinal sections of roots in Figure 4c further illustrated differences in endophytic colonization. Abundant fungal conidia (highlighted in red boxes) were observed inside root tissues, accompanying vigorous root growth in STH-treated plants. In the PTH-treated group, no fungal hyphae or conidia were detected within root cortical cells. The sparse hyphae present on the root surface failed to penetrate the intercellular spaces for stable endophytic colonization and only induced slight wrinkling of cell walls. Root cortical cells of untreated roots were tightly arranged with smooth, intact cell walls, and no hyphae or conidia were found. Collectively, these observations show more abundant fungal structures associated with root tissues under STH treatment relative to those under other treatments, and these structures were putatively identified morphologically as conidia of TH10. Notably, SEM observations only provide qualitative morphological evidence. Quantitative CFU-based enumeration of root colonization will be performed in future studies.

#### 3.3.3. Comparative Transcriptomic Profiling of Diseased Rice Tissues Under Strain TH10 Colonization

Transcriptome sequencing was used to explore the molecular mechanisms underlying STH-triggered alleviation of rice blast stress and to analyze SMS functions through genome-wide transcriptional and metabolic alterations. During the rice jointing stage, 32,225 expressed genes (FPKM > 0) were detected in root tissues and 31,404 in leaves among untreated, PTH and STH treatments. Inoculation with strain TH10, either alone or combined with SMS, did not alter the total number of expressed genes in rice roots and leaves. However, differentially expressed genes (DEGs) were identified using unified thresholds of an adjusted $p$-value (padj/FDR) < 0.05 and $|\log_2(\text{fold change})| \geq 1.0$. Venn diagrams were plotted to compare treatment-specific and shared expressed gene sets among the three treatment groups.

For root transcriptomes, as shown in Figure 5a, 17,929 genes (83.07%) were expressed in all three treatments. The numbers of treatment-specific expressed genes were 1 236 (5.73%) for the untreated control, 359 (1.66%) for PTH and 349 (1.62%) for STH. The number of overlapping expressed genes was the highest between STH and the untreated-control group (906). A total of 495 expressed genes were shared between STH and PTH, whereas only 310 overlapping genes existed between the untreated control and PTH. Based on the above Venn-derived expression profiles, KEGG pathway enrichment analysis was further performed on root DEGs of STH-treated rice, with the PTH treatment serving as the comparator. Seventeen significantly enriched pathways in roots were identified as illustrated in Figure 5b. Root tissues exhibited distinct enrichment patterns dominated by the upregulation of defense-related pathways and structural component biosynthesis pathways. Diterpenoid biosynthesis (dosa00904, $p < 0.001$), photosynthesis (dosa00195, $p < 0.001$), cutin, suberine, and wax biosynthesis (dosa00073, $p < 0.001$), as well as photosynthesis-antenna proteins (dosa00196, $p < 0.001$), were the most significantly upregulated pathways in roots. These pathways may support the formation of root epidermal physical barri-

ers, terpenoid phytoalexin synthesis, and intracellular DNA damage repair. By contrast, numerous pathways displayed significant downregulation in root tissues. Glucosinolate biosynthesis (dosa00966, $p < 0.01$) showed the most prominent downregulated enrichment. Meanwhile, plant-pathogen interaction (dosa04626, $p < 0.001$) and glycerolipid metabolism (dosa00561, $p < 0.01$) were all significantly suppressed.

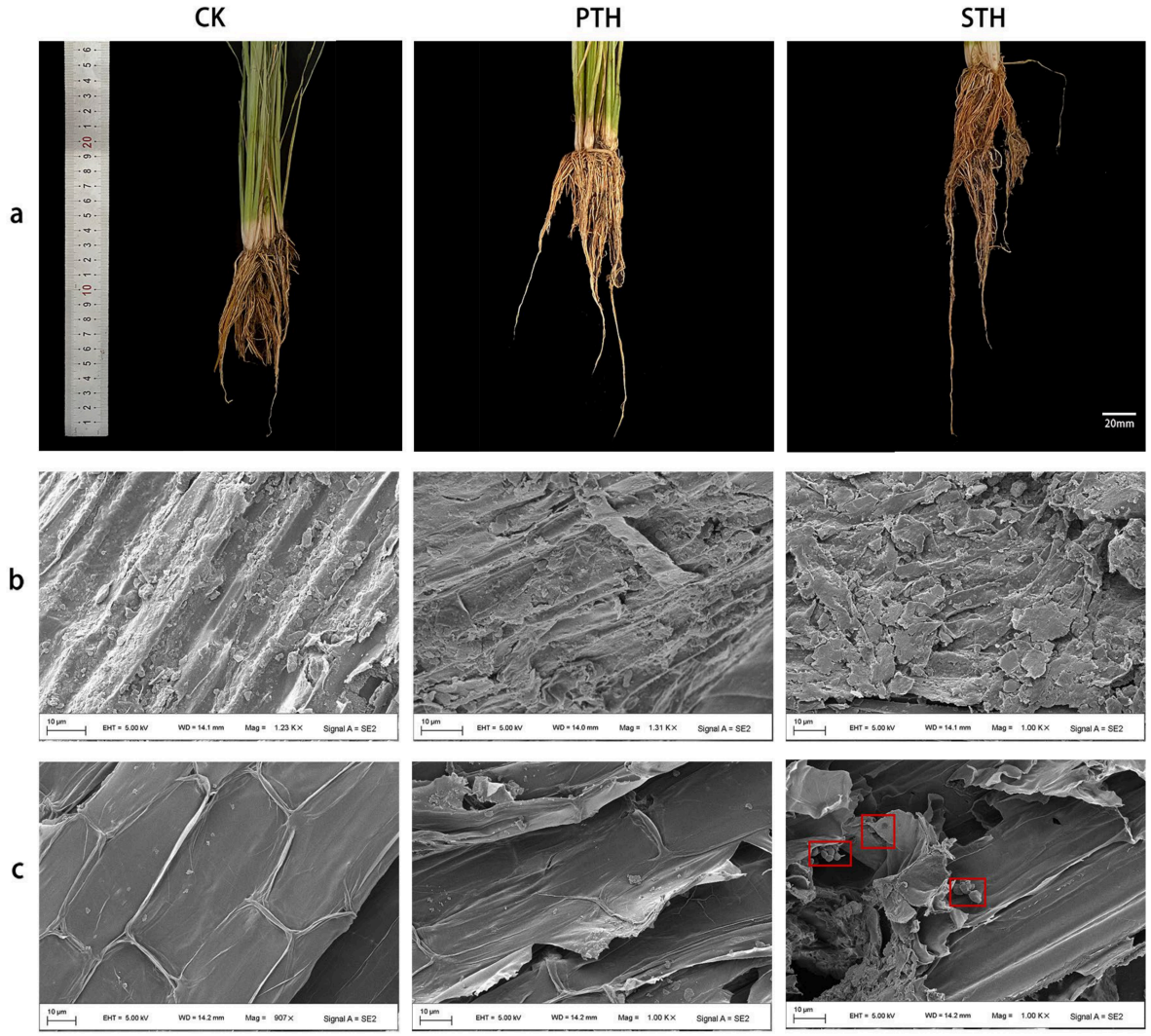



**Figure 4.** Comparison of rice root growth status and strain TH10 colonization at the tillering stage. (**a**) Comparison of rice root growth status, scale bar = 10 mm; (**b**) SEM images of the root epidermis, scale bar = 10 μm; (**c**) SEM images of longitudinal sections from rice root tissues, red boxes highlight conidia of strain TH10, scale bar = 10 μm. CK, untreated control roots; PTH, roots treated with strain TH10 powder; STH, roots treated with SMS-based TH10 inoculant. All experiments were performed with three biological replicates.

For leaf transcriptomes shown in Figure 5c, 18,515 genes (88.07%) were expressed across all treatments. Treatment-specific expressed genes numbered 318 (1.51%) in untreated, 357 (1.70%) in PTH and 674 (3.21%) in STH. Genes shared by two treatments included 579 between untreated control and PTH, 244 between untreated control and STH, and 335 between PTH and STH. Collectively, STH and PTH brought about only modest changes in leaf transcriptional profiles, and the proportion of commonly expressed genes in leaves was higher than that in roots. However, the proportion of STH treatment-specific expressed genes in leaves was higher than that in roots (3.21% in leaves versus 1.62% in roots). Among these unique genes, several hub genes with significant expression differences that participate in

plant immunity, hormone signaling and stress-response pathways, including *OsPR1* and *OsNPR1*, will be further analyzed in subsequent studies. Unlike the metabolic suppression trend observed in root samples, leaf tissues exhibited a divergent KEGG enrichment profile illustrated in Figure 5d. Plant hormone signal transduction (dosa04075, $p < 0.001$), plant-pathogen interaction (dosa04626, $p < 0.001$), and MAPK signaling pathway-plant (dosa04016, $p < 0.001$) were the most significantly upregulated pathways. Upregulation of these immune-related signaling cascades may underpin systemic stress responses and disease resistance in leaf tissues. In contrast, photosynthesis (dosa00195, $p < 0.001$), photosynthesis-antenna proteins (dosa00196, $p < 0.001$), glutathione metabolism (dosa00480, $p < 0.001$), biosynthesis of various plant secondary metabolites (dosa00999, $p < 0.001$), ABC transporters (dosa02010, $p < 0.001$), and flavone and flavonol biosynthesis (dosa00944, $p < 0.001$) were significantly downregulated. These results suggest leaves may prioritize stress resistance over photosynthetic carbon fixation while fine-tuning metabolic and energy allocation under the treatment, as presented in Figure 5d (Supplementary Data S3).

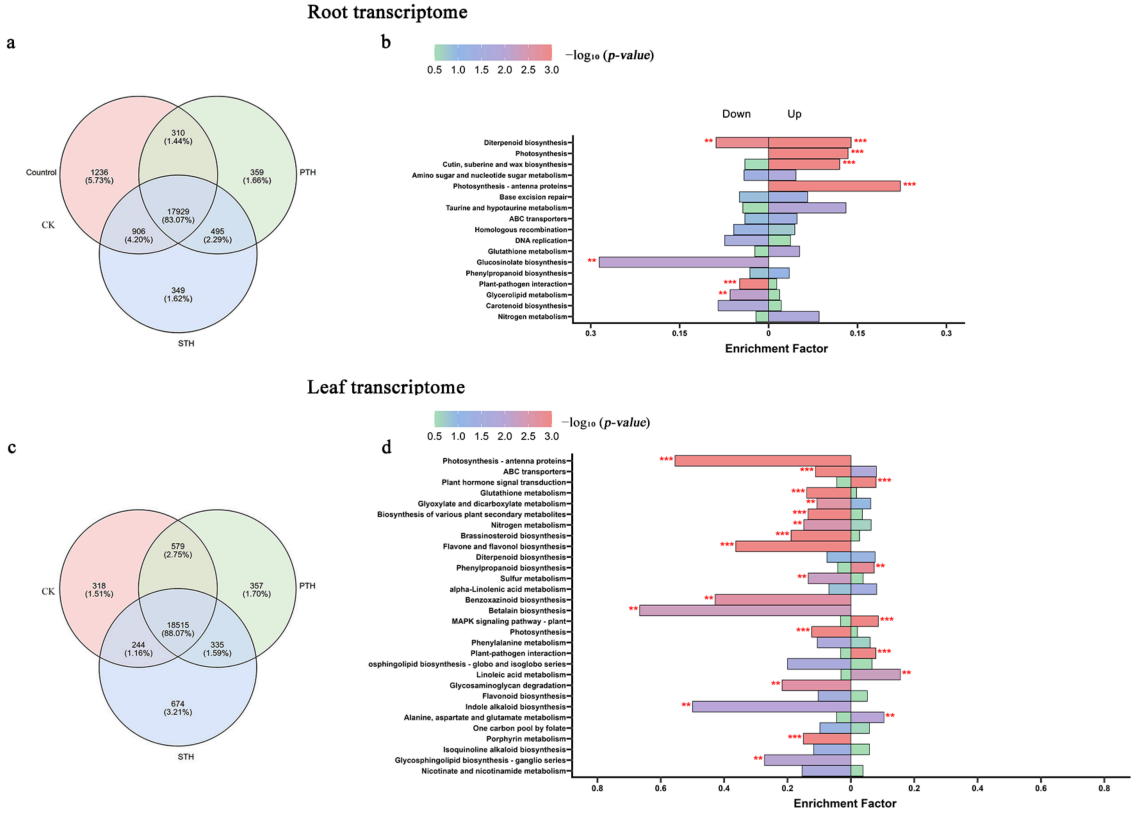



**Figure 5.** Comparative transcriptomic profiling of root and leaf tissues in diseased rice. (**a**) Venn diagram of expressed genes (FPKM > 0) in rice roots; (**b**) KEGG pathway enrichment of differentially expressed genes in rice roots, with the PTH treatment serving as the comparator; (**c**) Venn diagram of expressed genes (FPKM > 0) in rice leaves; (**d**) KEGG pathway enrichment of differentially expressed genes in rice leaves, with the PTH treatment serving as the comparator. Color gradient denotes $-\log_{10}$ (*p*-value), with red representing the highest enrichment significance, followed by purple and green in descending order. CK, untreated control roots; PTH, roots treated with strain TH10 powder; STH, roots treated with SMS-based TH10 inoculant. ** $p < 0.01$, *** $p < 0.001$. All experiments were performed with three biological replicates.

### 3.3.4. SMS-Mediated Effects of Strain TH10 on Endogenous Phytohormones

From comparative transcriptomic profiles, KEGG enrichment revealed plant-hormone signal transduction genes were significantly upregulated in rice leaves ($p < 0.001$). Variations in endogenous plant-hormone contents were further detected to verify transcriptional

results and clarify the connection between phenotypic differences and physiological responses. As key stress-responsive phytohormones, endogenous salicylic acid (SA), abscisic acid (ABA), and gibberellin $A_3$ ($GA_3$) in rice shoots, which individually mediate antioxidant defense, govern stomatal closure, and modulate stress-damage relief and growth recovery, were quantified by high-performance liquid chromatography (HPLC, 254 nm for ABA, 210 nm for SA/$GA_3$; chromatograms in Figure S4) at the seedling, tillering, and jointing stages [39–41]. All rice seedlings from the same batch were used for comparative experiments. The basal contents of SA, ABA and $GA_3$ in the untreated-control plants (CK) were 14.727 ± 2.075 μg/g, 12.503 ± 0.989 μg/g and 7.619 ± 0.371 μg/g, respectively, as presented in Figure 6.

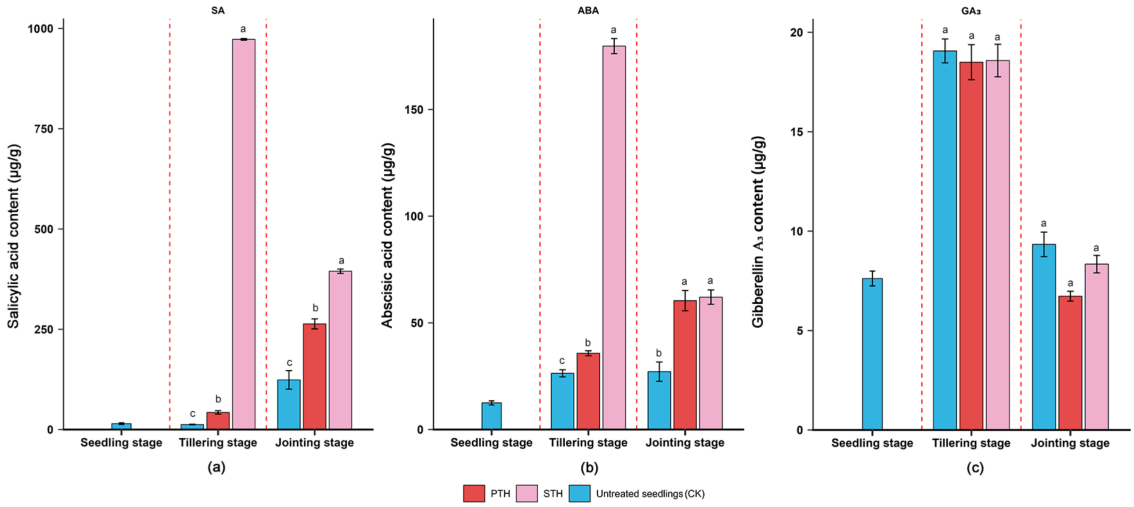



**Figure 6.** Determination of endogenous phytohormones in rice at seedling, tillering and jointing stages. (**a**) The content of salicylic acid (SA); (**b**) The content of abscisic acid (ABA); (**c**) The content of gibberellin $A_3$ (GA3). Blue bars: untreated control (CK); red bars: PTH treatment; pink bars: STH treatment. Red dotted lines separate different rice growth stages. Data are presented as means ± SD ($n$ = 3 biological replicates). Different letters indicate significant differences at each stage according to one-way ANOVA with Duncan's test ($p < 0.05$).

The results measured at the tillering stage showed that SA and ABA contents were significantly higher in the STH treatment than in CK and PTH. Specifically, SA and ABA concentrations in STH reached 972.750 ± 2.062 μg/g and 179.707 ± 3.540 μg/g, respectively, far exceeding those in CK and PTH. As shown in Figure 6c, $GA_3$ concentrations only slightly varied among the three groups, with CK at 19.063 ± 0.600 μg/g, PTH at 18.495 ± 0.890 μg/g and STH at 18.580 ± 0.818 μg/g. These hormone alterations coincided with *P. oryzae* Guy11 infection and root-associated fungal structures observed under STH treatment at the tillering stage. At the jointing stage, SA and ABA contents were significantly higher in the STH treatment than in CK and PTH. ABA levels of PTH were close to those of STH and both exceeded those in CK. SA, ABA and $GA_3$ concentrations all declined relative to their levels at the tillering stage. $GA_3$ concentrations also did not differ significantly among the three groups. Compared with tillering-stage hormone levels, all detected hormones decreased among the three groups. Collectively, STH-treated rice shoots exhibited significantly higher SA and ABA accumulation compared with PTH. Following the overall decrease in $GA_3$ from the tillering stage, no significant differences were observed among CK, PTH and STH treatments (Supplementary Data S4).

## 4. Discussion

*Trichoderma harzianum* is limited in field-scale application as a biocontrol inoculant due to its limited ability to colonize rice roots. In this study, greenhouse assays suggested that SMS, as a carrier, may promote the formation of root-associated fungal structures and enhance rice-blast biocontrol efficacy of *T. harzianum* strain TH10 isolated from marine algal sediments. SEM observations revealed extensive hyphal networks on the root surface and abundant conidia inside root tissues under STH treatment. In contrast, under the PTH treatment, only a small number of fungal hyphae loosely adhered to the root epidermis. These hyphae could not maintain persistent presence in the rhizosphere and failed to penetrate internal tissues to establish stable endophytic colonization. This result is consistent with the report by David et al. [42] that *Trichoderma* applied without an organic carrier rapidly loses viability owing to antagonism by native soil microorganisms and fails to persist in the rhizosphere. Variations in rhizosphere microenvironment may affect rice growth and defense responses, which may be associated with the significant differences in root architecture and panicle-blast control efficacy between STH and PTH.

Greenhouse experiments revealed that, compared with PTH, STH persistently promoted rice root elongation by 15.87–29.51% and total biomass accumulation by 4.91–13.93% across the three-leaf, tillering, jointing and maturity stages, and improved root dry weight by 16.70% and 1000-grain weight by 12.99% at maturity. Previous studies have demonstrated that SMS is rich in organic matter, polysaccharides and secondary metabolites, and its decomposition continuously releases small-molecule organic acids, humic acids and humic substances, thereby increasing the pools of AN, AP and AK in paddy soils [43,44]. Such organic amendments can reduce soil salinity [45]. Therefore, the fertility improvement observed under STH treatment cannot be simply attributed to direct nutrient supplementation. In the present study, an additional SMS-only control was included for rhizosphere soil physicochemical evaluation, which helped to partially distinguish soil property changes originating from the SMS itself. As confirmed by rhizosphere soil analyses of four SMS-based TH10 treatments, bioactive substances released during SMS degradation elevated soil OM, AN, AP and AK pools by 177.78–814.43%, 1632.22–2764.77%, 3258.54–6310.19% and 517.85–1015.50%, respectively, and reduced soil total-salt content by 5.25–72.20%. These results explain the improved root growth and yield traits under *P. oryzae* Guy11-induced stress. STH establishes a favorable rhizosphere microenvironment for root elongation and lateral-root formation, which is consistent with the increased root dry weight and persistent root-growth promotion by STH across rice developmental stages.

SEM observations revealed fungal hyphae on rice root surfaces, presumed to represent TH10. Microscopic interaction studies by Giordano et al. [46] confirmed that stable endophytic colonization by *T. harzianum* ITEM 3636 is essential for triggering induced systemic resistance in host plants. Similarly, in planta biocontrol assays against rice blast caused by *P. oryzae* Guy11 revealed that STH reduced panicle-blast severity to 14.60 $\pm$ 2.68% and achieved a greenhouse biocontrol efficacy of 51.34 $\pm$ 6.39%, decreased the rate of withered grains by 51.89%, and increased the seed-setting rate to 85.40 $\pm$ 2.68%. Dual-culture assays and SEM images indicated that strain TH10 suppresses *P. oryzae* Guy11 primarily by secreting inhibitory metabolites. The $EC_{50}$ was achieved at a 1.262 $\times$ $10^3$-fold dilution of the cell-free supernatant.

Comparative transcriptomic profiling further confirmed that SMS promotes strain TH10's agronomic and biocontrol performance, revealing that STH did not alter the global transcriptional profile in rice roots and leaves, but rather enhanced tissue-specific defense responses. In leaves, activation of MAPK cascades (dosa04016) and plant hormone signal transduction (dosa04075) initiated systemic above-ground immunity against foliar infection. This enhancement of tissue-specific defense responses was also reflected in the significant downregulation

of photosynthetic pathways, whereby rice temporarily reduced carbon assimilation to redirect metabolic resources toward immune activation. Such metabolic reprogramming may be triggered by *Trichoderma*-mediated defense priming that is positively correlated with its root-colonization density [47,48]. In roots, the significantly upregulated biosynthesis of cutin, suberin and wax (dosa00073), which may be stimulated by fungal mycelia released from SMS, may support fungal growth on rice roots. The tissue-specific defense responses were manifested in significant accumulation of diterpenoid phytoalexins (dosa00904).

In addition, transcriptome sequencing revealed that the majority of genes involved in plant hormone signal transduction were significantly upregulated (Supplementary Data S5). Endogenous hormone quantification results verified the transcriptional changes in hormone signal pathways. At the tillering stage, with Guy11 inoculated onto the tiller nodes and STH applied by root-hole placement, SA and ABA contents in rice shoots increased to 972.750 ± 2.062 μg/g and 179.707 ± 3.540 μg/g, which were markedly higher than those in the untreated control and PTH treatments. This phenomenon suggests that rhizosphere changes induced by SMS application may facilitate the transmission of defense signals to above-ground tissues. SA regulates rice resistance against Guy11, and ABA improves multi-stress tolerance in rice. No significant differences in $GA_3$ concentrations were observed among treatments, indicating that the growth-promoting and biocontrol effects of STH were not mediated by $GA_3$-dependent regulation, but potentially relied on SA- and ABA-related defense pathways. Nevertheless, we emphasize that changes in endogenous phytohormone levels alone cannot provide conclusive genetic evidence for hormone-mediated resistance. This is consistent with a previous study by Shasmita et al. [49], which reported that *Trichoderma* colonization can enhance the accumulation of both SA and ABA in rice tissues, thereby activating defense responses against pathogens. The transcriptomic data provide correlative evidence of rice molecular responses, and the proposed regulatory mechanisms remain hypothetical and require further functional validation.

## 5. Conclusions

In this study, we found that SMS can act as a promising carrier for *T. harzianum* TH10, improving rice growth and panicle-blast resistance. This may be attributed to SMS supplying nutrients to support the formation of root-associated fungal structures, while potentially providing protective microenvironments that alleviate competitive pressure from resident rhizosphere microbes. These hypotheses, however, require further quantitative assays and microbiome analyses in future work. Furthermore, transcriptome sequencing revealed that the combination of SMS and strain TH10 could activate tissue-specific defensive reactions and may contribute to increasing the accumulation of SA and ABA, which enhances host responses to rice blast. Compared with strain TH10 powder, the STH significantly promoted root development, vegetative growth and tillering, ultimately decreasing panicle-blast severity and improving yield-related traits. Based on these findings, future studies will further explore how strain TH10 modulates SA- and ABA-related defense pathways using RT-qPCR and multi-omics analysis, and characterize the corresponding downstream defense-related metabolic pathways, which may facilitate the practical application of SMS-based biocontrol agents in sustainable agricultural production.

## 6. Limitations of the Study

The present study has several limitations that should be acknowledged. First, the absence of an SMS-only treatment constitutes the major experimental limitation. The original experimental design primarily aimed to evaluate whether SMS could improve the field performance of *T. harzianum* TH10, rather than to characterize the independent biological functions of SMS. Therefore, phenotypic, phytohormonal, and transcriptomic

data corresponding to the sole SMS treatment were not collected in the current experimental cycle. Second, root colonization of TH10 was only qualitatively observed via SEM, without quantitative CFU enumeration, which limits the quantitative interpretation of colonization capacity. In addition, the mechanistic associations among SMS carrier effects, strain colonization, SA and ABA signaling, and rice blast resistance proposed in this study remain preliminary and speculative and cannot be fully validated by the current datasets. Future work will incorporate independent SMS treatments, quantitative colonization assays, and multi-omics verification to disentangle substrate-derived and strain-mediated effects and further validate the underlying defense regulatory mechanisms.

**Supplementary Materials:** The following supporting information can be downloaded at: https://www.mdpi.com/article/10.3390/microorganisms14112420/s1, Supplementary Data S1: Source data for $EC_{50}$ determination of TH10 cell-free culture supernatant against *Pyricularia oryzae*; Data S2: Soil physicochemical properties under different SMS-based TH10 treatments; Data S3-1: Enriched KEGG pathways from root transcriptomes; Data S3-2: Enriched KEGG pathways from leaf transcriptomes; Data S4-1: Phytohormone contents of rice at different growth stages under various treatments; Data S4-2: Standard curve data for salicylic acid (SA), abscisic acid (ABA) and gibberellin $A_3$ ($GA_3$) using HPLC; Data S5-1: Source data of SMS-based TH10 (STH) soil application effect on root transcription in rice blast infected plants; Data S5-2: Source data of SMS-based TH10 (STH) inoculant soil application effect on leaf transcription in rice blast infected plants; Data S5-3: Summary of RNA-seq quality control and DEG statistics for rice root and leaf samples; Table S1. Strains and plant materials used in this study; Table S2. Source data for detached rice-leaf assays of TH10 against Guy 11; Figure S1. Schematic diagram of greenhouse pot experiment for rice; Figure S2. Antifungal effects of *T. harzianum* TH10 cell-free filtrate against Guy11; Figure S3. Growth and panicle morphologies of rice plants under CK, PTH and STH treatments; Figure S4. Representative HPLC chromatograms of the phytohormone standard mixture and rice-leaf extract.

**Author Contributions:** N.L. designed and performed the experiments, and drafted the initial manuscript. N.L. and X.C. contributed equally. H.Z. participated in the experimental design and analysis of experimental results. M.Y. and M.L. conceived and supervised the project, and guided the experimental design, data analysis, manuscript writing and revision. All authors have read and agreed to the published version of the manuscript.

**Funding:** This research was funded by Tiankai Higher Education Science and Technology Innovation Park Enterprise R&D Special Project, grant number 23YFZXYC00019; Major Science and Technology Special Project of Tianjin 2024 Carbon Peak and Carbon Neutral, grant number 24ZXTKSN00080; Tianjin Key Research and Development Program CAS-Cooperation Project, grant number 24YFYSHZ00060.

**Institutional Review Board Statement:** Not applicable.

**Informed Consent Statement:** Not applicable.

**Data Availability Statement:** The transcriptome raw data have been deposited in the Genome Sequence Archive (GSA) under accession number PRJCA075502. Other data are available in the manuscript and Supplementary Materials.

**Acknowledgments:** We sincerely thank the Henan Academy of Agricultural Sciences, China, for providing the rice cultivar Zhenghan 10, and Henan Yuxin Edible Mushroom Planting Professional Cooperative, China, for supplying all SMS materials.

**Conflicts of Interest:** The authors declare no conflicts of interest.

## References

1. Jukanti, A.K.; Karapati, D.; Bharali, V.; Gudla, M.; Thati, S.; Yadla, S.; Kumar, M.; Sundaram, R.M. From gene to plate: Molecular insights into and health implications of rice (*Oryza sativa* L.) grain protein. *Int. J. Mol. Sci.* **2025**, *26*, 3163. [CrossRef]

2. Kabore, M.A.F.; Huang, G.; Feng, C.; Wu, S.; Guo, J.; Wu, G.; Sun, Y.; Woldegiorgis, S.T.; Ai, Y.; Zhang, L.; et al. *Piriformospora indica* enhances rice blast resistance and plant growth. *Agronomy* **2025**, *15*, 118. [CrossRef]
3. Guo, F.; Chen, X.; Lu, M.; Yang, L.; Wang, S.; Wu, B.M. Spatial analysis of rice blast in china at three different scales. *Phytopathology* **2018**, *108*, 1276–1286. [CrossRef]
4. Simkhada, K.; Thapa, R. Rice blast, a major threat to the rice production and its various management techniques. *Turk. J. Agric. Food Sci. Technol.* **2022**, *10*, 147–157. [CrossRef]
5. Asibi, A.E.; Chai, Q.; Coulter, J.A. Rice blast: A disease with implications for global food security. *Agronomy* **2019**, *9*, 451. [CrossRef]
6. Park, J.-Y.; Jin, J.; Lee, Y.-W.; Kang, S.; Lee, Y.-H. Rice blast fungus (*Magnaporthe oryzae*) infects arabidopsis via a mechanism distinct from that required for the infection of rice. *Plant Physiol.* **2009**, *149*, 474–486. [CrossRef]
7. Dean, R.A.; Talbot, N.J.; Ebbole, D.J.; Farman, M.L.; Mitchell, T.K.; Orbach, M.J.; Thon, M.; Kulkarni, R.; Xu, J.-R.; Pan, H. The genome sequence of the rice blast fungus *Magnaporthe grisea*. *Nature* **2005**, *434*, 980–986. [CrossRef]
8. Couch, B.C.; Kohn, L.M. A multilocus gene genealogy concordant with host preference indicates segregation of a new species, *Magnaporthe oryzae*, fromm. *Grisea. Mycol.* **2017**, *94*, 683–693. [CrossRef]
9. Fernandez, J.; Orth, K. Rise of a cereal killer: The biology of *Magnaporthe oryzae* biotrophic growth. *Trends Microbiol.* **2018**, *26*, 582–597. [CrossRef]
10. Devkota, S.R.Y. A review on various management method of rice blast disease. *Malays. J. Sustain. Agric.* **2020**, *4*, 29–33. [CrossRef]
11. Gupta, L.; Vermani, M.; Kaur Ahluwalia, S.; Vijayaraghavan, P. Molecular virulence determinants of *Magnaporthe oryzae*: Disease pathogenesis and recent interventions for disease management in rice plant. *Mycology* **2021**, *12*, 174–187. [CrossRef]
12. Woo, S.L.; Hermosa, R.; Lorito, M.; Monte, E. *Trichoderma*: A multipurpose, plant-beneficial microorganism for eco-sustainable agriculture. *Nat. Rev. Microbiol.* **2022**, *21*, 312–326. [CrossRef]
13. Song, Y.-P.; Ji, N.-Y. Chemistry and biology of marine-derived *Trichoderma* metabolites. *Nat. Prod. Bioprospect.* **2024**, *14*, 14. [CrossRef]
14. Jiang, M.; Wu, Z.; Guo, H.; Liu, L.; Chen, S. A review of terpenes from marine-derived fungi: 2015–2019. *Mar. Drugs* **2020**, *18*, 321. [CrossRef]
15. Li, H.; Liu, X.; Li, X.; Hu, Z.; Wang, L. Novel harziane diterpenes from deep-sea sediment fungus *Trichoderma* sp. Scsiow21 and their potential anti-inflammatory effects. *Mar. Drugs* **2021**, *19*, 689. [CrossRef]
16. Harman, G.E.; Howell, C.R.; Viterbo, A.; Chet, I.; Lorito, M. *Trichoderma* species—Opportunistic, avirulent plant symbionts. *Nat. Rev. Microbiol.* **2004**, *2*, 43–56. [CrossRef]
17. Yang, X.; Chen, L.; Yong, X.; Shen, Q. Formulations can affect rhizosphere colonization and biocontrol efficiency of *Trichoderma harzianum* sqr-t037 against fusarium wilt of cucumbers. *Biol. Fertil. Soils* **2010**, *47*, 239–248. [CrossRef]
18. Basińska-Barczak, A.; Błaszczyk, L.; Szentner, K. Plant cell wall changes in common wheat roots as a result of their interaction with beneficial fungi of *Trichoderma*. *Cells* **2020**, *9*, 2319. [CrossRef]
19. Yeats, T.H.; Rose, J.K.C. The formation and function of plant cuticles. *Plant Physiol.* **2013**, *163*, 5–20. [CrossRef]
20. Chen, A.; Liu, T.; Wang, Z.; Chen, X. Plant root suberin: A layer of defence against biotic and abiotic stresses. *Front. Plant Sci.* **2022**, *13*, 1056008. [CrossRef]
21. Mariola, R.; Chacon, O.; Tahia, B.; Sonia, S.; Manuel, R.; Antoniomm, L.; Jesus, D. Microscopic and transcriptome analyses of early colonization of tomato roots by *Trichoderma harzianum*. *Int. Microbiol.* **2007**, *10*, 19–27. [CrossRef]
22. Hermosa, R.; Viterbo, A.; Chet, I.; Monte, E. Plant-beneficial effects of *Trichoderma* and of its genes. *Microbiology* **2012**, *158*, 17–25. [CrossRef]
23. Alfiky, A.; Weisskopf, L. Deciphering *Trichoderma*–plant–pathogen interactions for better development of biocontrol applications. *J. Fungi* **2021**, *7*, 61. [CrossRef]
24. Chen, L.; Zhou, W.; Luo, L.; Li, Y.; Chen, Z.; Gu, Y.; Chen, Q.; Deng, O.; Xu, X.; Lan, T.; et al. Short-term responses of soil nutrients, heavy metals and microbial community to partial substitution of chemical fertilizer with spent mushroom substrates (SMS). *Sci. Total Environ.* **2022**, *844*, 157064. [CrossRef]
25. Iglesias, H.; Ortiz, A.P.; Soriano Disla, J.M.; Lara-Guillén, A.J. Environmental and economic life cycle impacts of using spent mushroom substrate as a soil improver. *Environments* **2025**, *12*, 31. [CrossRef]
26. Yuan, Y.; Yu, X.; Jiang, Q.; Zhao, C.; Cheng, Z. Study on cultivation of *Trichoderma viride* using spent mushroom substrate and control effect on soybean root rot. *J. Mater. Cycles Waste Manag.* **2022**, *24*, 1524–1532. [CrossRef]
27. Xiao, Z.; Zhao, Q.; Li, W.; Gao, L.; Liu, G. Strain improvement of *Trichoderma harzianum* for enhanced biocontrol capacity: Strategies and prospects. *Front. Microbiol.* **2023**, *14*, 1146210. [CrossRef]
28. Gutiérrez-Moreno, K.; Olguín-Martínez, A.I.; Montoya-Martínez, A.C.; de los Santos-Villalobos, S. *Trichoderma* in sustainable agriculture and the challenges related to its effectiveness. *Diversity* **2025**, *17*, 734. [CrossRef]
29. dos Santos, J.M.R. Underground warfare: Mechanisms of *Trichoderma* in the suppression of the march of fusarium in banana plants—Advances, limitations and perspectives. *J. Phytopathol.* **2025**, *173*, e70205. [CrossRef]

30. Zhang, C.; Wang, W.; Hu, Y.; Peng, Z.; Ren, S.; Xue, M.; Liu, Z.; Hou, J.; Xing, M.; Liu, T. A novel salt-tolerant strain *Trichoderma atroviride* hn082102.1 isolated from marine habitat alleviates salt stress and diminishes cucumber root rot caused by *Fusarium oxysporum*. *BMC Microbiol.* **2022**, *22*, 67. [CrossRef]
31. Naeimi, S.; Khosravi, V.; Varga, A.; Vágvölgyi, C.; Kredics, L. Screening of organic substrates for solid-state fermentation, viability and bioefficacy of *Trichoderma harzianum* as12-2, a biocontrol strain against rice sheath blight disease. *Agronomy* **2020**, *10*, 1258. [CrossRef]
32. Vardar, F.; Eltem, R.; GezgİN, Y.; Sargin, S. Micropropagule production from *Trichoderma harzianum* ege-k38 using solid-state fermentation and a comparative study for drying methods. *Turk. J. Biol.* **2013**, *27*, 139–146. [CrossRef]
33. Aiduang, W.; Jatuwong, K.; Kiatsiriroat, T.; Kamopas, W.; Tiyayon, P.; Jawana, R.; Xayyavong, O.; Lumyong, S. Spent mushroom substrate-derived biochar and its applications in modern agricultural systems: An extensive overview. *Life* **2025**, *15*, 317. [CrossRef]
34. Kumar, V.; Singh, P.K.; Karkute, S.G.; Tasleem, M.; Bhagat, S.; Abdin, M.Z.; Sevanthi, A.M.; Rai, A.; Sharma, T.R.; Singh, N.K.; et al. Identification of novel resources for panicle blast resistance from wild rice accessions and mutants of cv. Nagina 22 by syringe inoculation under field conditions. *3 Biotech* **2022**, *12*, 53. [CrossRef]
35. Sparks, D.L.; Page, A.L.; Helmke, P.A.; Loeppert, R.H.; Soltanpour, P.N.; Tabatabai, M.A.; Johnston, C.T.; Sumner, M.E. *Methods of Soil Analysis: Part 3 Chemical Methods*; John Wiley & Sons: Hoboken, NJ, USA, 1996. [CrossRef]
36. Prismantoro, D.; Jefferson, T.A.; Akbari, S.I.; Miranti, M.; Mispan, M.S.; Doni, F. In vitro inhibition mechanisms of *Trichoderma yunnanense* tm10 against *Pyricularia oryzae* and *Rhizoctonia solani* causing blast and sheath blight diseases in rice (*Oryza sativa* L.). *All. Life* **2024**, *17*, 2422845. [CrossRef]
37. Vinale, F.; Sivasithamparam, K.; Ghisalberti, E.L.; Woo, S.L.; Nigro, M.; Marra, R.; Lombardi, N.; Pascale, A.; Ruocco, M.; Lanzuise, S.; et al. *Trichoderma* secondary metabolites active on plants and fungal pathogens. *Open Mycol. J.* **2014**, *8*, 127–139. [CrossRef]
38. Nguyen, Q.T.; Ueda, K.; Kihara, J.; Ueno, M. Culture filtrates of *Trichoderma* isolate H921 inhibit *Magnaporthe oryzae* spore germination and blast lesion formation in rice. *Adv. Microbiol.* **2016**, *06*, 521–527. [CrossRef]
39. Hussain, S.; Nanda, S.; Ashraf, M.; Siddiqui, A.; Masood, S.; Khaskheli, M.; Suleman, M.; Zhu, L.; Zhu, C.; Cao, X.; et al. Interplay impact of exogenous application of abscisic acid (aba) and brassinosteroids (brs) in rice growth, physiology, and resistance under sodium chloride stress. *Life* **2023**, *13*, 498. [CrossRef]
40. Li, X.; Xiao, L.; Song, Y.; Wei, X.; Rengel, Z.; Chen, Y.; Li, K.; Chen, Q. Coordination of phytomelatonin and salicylic acid signalling in stomatal closure. *Plant Cell Environ.* **2025**, *48*, 7656–7670. [CrossRef]
41. Tripathi, J.M.; Khan, B.R.; Gaur, R.; Yadav, D.; Verma, K.K.; Gupta, R. Gibberellic acid improves photosynthetic electron transport and stomatal function in crops that are adversely affected by salinity exposure. *Plants* **2025**, *14*, 3388. [CrossRef]
42. Ruano-Rosa, D.; Prieto, P.; Rincón, A.M.; Gómez-Rodríguez, M.V.; Valderrama, R.; Barroso, J.B.; Mercado-Blanco, J. Fate of *Trichoderma harzianum* in the olive rhizosphere: Time course of the root colonization process and interaction with the fungal pathogen *Verticillium dahliae*. *BioControl* **2015**, *61*, 269–282. [CrossRef]
43. Tang, Q.; Liu, W.; Huang, H.; Peng, Z.; Deng, L. Responses of crop yield, soil fertility, and heavy metals to spent mushroom residues application. *Plants* **2024**, *13*, 663. [CrossRef]
44. Jumar, J.; Saputra, R.A.; Nugraha, M.I.; Wahyudianur, A. Essential dynamics of rice cultivated under intensification on acid sulfate soils ameliorated with composted oyster mushroom baglog waste. *Pertanika J. Trop. Agric. Sci.* **2022**, *45*, 565–586. [CrossRef]
45. Martín, C.; Zervakis, G.I.; Xiong, S.; Koutrotsios, G.; Strætkvern, K.O. Spent substrate from mushroom cultivation: Exploitation potential toward various applications and value-added products. *Bioengineered* **2023**, *14*, 2138. [CrossRef]
46. Giordano, D.F.; Pastor, N.A.; Rouws, L.F.M.; de Freitas, K.M.; Erazo, J.G.; Del Canto, A.; da Silva Coelho, I.; Oddino, C.M.; Torres, A.M. *Trichoderma harzianum* item 3636 colonizes peanut roots as an endophyte and protects the plants against late leaf spot. *Symbiosis* **2023**, *89*, 337–352. [CrossRef]
47. Meng, Q.; Gupta, R.; Kwon, S.J.; Wang, Y.; Agrawal, G.K.; Rakwal, R.; Park, S.-R.; Kim, S.T. Transcriptomic analysis of *Oryza sativa* leaves reveals key changes in response to *Magnaporthe oryzae* msp1. *Plant Pathol. J.* **2018**, *34*, 257–268. [CrossRef]
48. Cohen, S.P.; Leach, J.E. Abiotic and biotic stresses induce a core transcriptome response in rice. *Sci. Rep.* **2019**, *9*, 6273. [CrossRef]
49. Shasmita; Hota, S.; Mukherjee, A.K.; Naik, S.K.; Mohapatra, P.K. Priming with *Trichoderma* for induction of defense against rice pathogens. *Cereal Res. Commun.* **2025**, *54*, 1–24. [CrossRef]


**Disclaimer/Publisher's Note:** The statements, opinions and data contained in all publications are solely those of the individual author(s) and contributor(s) and not of MDPI and/or the editor(s). MDPI and/or the editor(s) disclaim responsibility for any injury to people or property resulting from any ideas, methods, instructions or products referred to in the content.